Original Article

MOLECULAR METABOLISM

Atlas of exercise-induced brain activation in mice

Grethe Skovbjerg[1,2], Andreas Mæchel Fritzen[3,4], Charlotte Sashi Aier Svendsen[1], Johanna Perens[2], Jacob Lercke Skytte[2], Camilla Lund[1], Jens Lund[1], Martin Rønn Madsen[2], Urmas Roostalu[2], Jacob Hecksher-Sørensen[2], Christoffer Clemmensen[1,*,5]

ABSTRACT

Objectives: There is significant interest in uncovering the mechanisms through which exercise enhances cognition, memory, and mood, and lowers the risk of neurodegenerative diseases. In this study, we utilize forced treadmill running and distance-matched voluntary wheel running, coupled with light sheet 3D brain imaging and c-Fos immunohistochemistry, to generate a comprehensive atlas of exercise-induced brain activation in mice.

Methods: To investigate the effects of exercise on brain activity, we compared whole-brain activation profiles of mice subjected to treadmill running with mice subjected to distance-matched wheel running. Male mice were assigned to one of four groups: a) an acute bout of voluntary wheel running, b) confinement to a cage with a locked running wheel, c) forced treadmill running, or d) placement on an inactive treadmill. Immediately following each exercise or control intervention, blood samples were collected for plasma analysis, and brains were collected for whole-brain c-Fos quantification.

Results: Our dataset reveals 255 brain regions activated by acute exercise in mice, the majority of which have not previously been linked to exercise. We find a broad response of 140 regulated brain regions that are shared between voluntary wheel running and treadmill running, while 32 brain regions are uniquely regulated by wheel running and 83 brain regions uniquely regulated by treadmill running. In contrast to voluntary wheel running, forced treadmill running triggers activity in brain regions associated with stress, fear, and pain.

Conclusions: Our findings demonstrate a significant overlap in neuronal activation signatures between voluntary wheel running and distance-matched forced treadmill running. However, our analysis also reveals notable differences and subtle nuances between these two widely used paradigms. The comprehensive dataset is accessible online at www.neuropedia.dk, with the aim of enabling future research directed towards unraveling the neurobiological response to exercise.

Keywords Exercise; Wheel running; Treadmill running; Brain activity; c-Fos; Stress

1. INTRODUCTION

Regular exercise is acknowledged for its wide-ranging benefits to brain health, including mood improvement and protection against age-related cognitive decline and neurodegenerative diseases [1—3]. As for long-term exercise training, a growing body of research also suggests a significant influence of a single bout of exercise, termed "acute exercise", on brain function, including enhancement of emotional states and stress coping [4]. In the context of exercise, the most widely studied brain region is arguably the hippocampus [5], but running wheel exercise in rodents coincides with neuronal activity in a long list of brain regions, including the hypothalamus [6], several striatal regions [7], the somatosensory cortex [6], the medial prefrontal cortex [8], and the motor-coordinating red nucleus of the midbrain [9]. Thus, not surprisingly, endurance exercise in rodents has been linked to pleiotropic central effects including effects on appetite, reward, pain, locomotion, and proprioception [10—15]. Insights into the impact of exercise on the brain have largely been derived from studies conducted on rats or mice, utilizing two commonly employed exercise paradigms: forced treadmill running and voluntary wheel running [16,17]. While forced treadmill running offers control over exercise intensity and duration, it has been implied to be a stressful paradigm [18,19]. Both male and female rats exhibit increased plasma corticosterone levels in response to treadmill running [20]. Accordingly, phenotypic changes resulting from forced treadmill running may be attributed not only to exercise itself but also to the added stress [20]. Running wheels, in contrast, are often viewed as an environmental enrichment [21] and rodents voluntarily engage with running wheels to run distances of 4—8 km each night, depending on strain and sex. This underscores that running wheels provide an opportunity for mice and rats to engage in

[1]Novo Nordisk Foundation Center for Basic Metabolic Research, Faculty of Health and Medical Sciences, University of Copenhagen, Copenhagen, Denmark [2]Gubra, Hørsholm, Denmark [3]August Krogh Section for Molecular Physiology, Department of Nutrition, Exercise and Sports, Faculty of Science, University of Copenhagen, Copenhagen, Denmark [4]Department of Biomedical Sciences, Faculty of Health and Medical Sciences, University of Copenhagen, Copenhagen, Denmark

[5] Lead contact.

*Corresponding author. E-mail: chc@sund.ku.dk (C. Clemmensen).

Received February 8, 2024 • Accepted February 25, 2024 • Available online 28 February 2024

https://doi.org/10.1016/j.molmet.2024.101907

regular exercise, and that this activity is remarkably rewarding for the animals [21,22]. Despite the substantial differences between these two endurance exercise interventions, they are often interchangeably utilized in the literature. This is potentially problematic, and the stressful aspects of forced treadmill running might limit the predictable value of this intervention for mimicking human exercise.

Previous attempts to understand the underlying mechanisms for exercise on brain health have focused on specific, pre-selected brain regions. However, given the intricacy of the brain and the diverse effects of exercise on brain health, a more global, unbiased approach is required to grasp the complete brain activation signature induced by exercise. Recent histological advancements combining tissue clearing and light-sheet fluorescent microscopy (LSFM) have enabled whole-brain mapping and quantification of neuronal activation patterns at single-cell resolution [23–30]. In this study, we take advantage of this methodological advancement, using c-Fos expression as an indicator of neuronal stimulation, to provide a comprehensive 3D analysis of whole-brain activity patterns in exercising male mice. We compare c-Fos response of forced treadmill running to distance-matched voluntary wheel running and scrutinize the confounding effects that can be attributed to exercise control groups. Finally, we have developed an online activity-induced brain map resource, available at www.neuropedia.dk, that can be used to guide and support future exploration into the neurological effects of exercise.

2. METHODS

2.1. Animals

All *in vivo* experiments were conducted at the University of Copenhagen, Denmark, according to internationally accepted principles for animal care and under approval from the Danish Animal Experiments Inspectorate, Danish Ministry of Food, Agriculture and Fisheries (permit number: 2018-15-0201-01457). The mice were single-housed in a temperature-controlled environment (21–23 °C) enriched with nesting materials on a 12:12-h light–dark cycle (light: 6:00 am - 6:00 pm; dark: 6:00 pm–6:00 am CEST) with *ad libitum* access to chow diet (Altromin 1324, Brogaarden, DK) and drinking water, unless otherwise specified. All *in vivo* experiments were conducted using male C57Bl/6J mice (Janvier, FR) at the age of 9–10 weeks. Minimum 1 week before study start, mice were habituated to single housing and randomized into four groups: treadmill control (CTRL-TR, n = 8), treadmill running (TR, n = 8), wheel running control (CTRL-WR, n = 8), and wheel running (WR, n = 25).

2.2. Treadmill acclimatization and exercise

Prior to the terminal treadmill exercise experiment, treadmill runners and treadmill control mice were all acclimatized to a treadmill running system (TSE Systems, GmbH, Germany). The adaptation protocol comprised 10 min at 10.2 m min^{-1} each day for three consecutive days (with active shocker grid), whereafter mice rested for two days prior to the day of termination to avoid any residual effects of acute exercise. On the day of termination, mice were exposed to a running paradigm of 10 min at 6 m min^{-1} then 40 min at 17.4 m min^{-1} (50% of max speed) followed by gradually increased speed (0.6 m min^{-1} every minute for 10 min - thereafter 1.8 m min^{-1} every minute) until exhaustion. All treadmill exercise performed at an incline of 10°. Mice were forced to run until exhaustion using pressurized air and an electric shocker grid at the back of the treadmill. Exhaustion was defined when mice fell back to the grid three times within 30 s. Treadmill controls were placed on an inactive treadmill for ~1 h on termination day. Treadmill habituation and exercise experiment was performed 1–3 h into the dark phase (zeitgeber time, ZT 13-16).

2.3. Running wheel acclimatization and exercise

Wheel running control and wheel running mice were single housed 12 days prior to termination in cages equipped with running wheels (23 cm in diameter, Techniplast activity cage, Techniplast, Buguggiate, Italy). Amount of bedding was reduced in order to avoid blocking of the running wheel. 5 days prior to termination, running wheels were unlocked and mice had free access to active running wheels for 2 days, followed by 3 days where running wheels were unlocked 2 h a day 1–3 h into the dark phase (ZT 13-16) to acclimatize the mice to the running wheels, but at the same time avoid exercise training effects prior to the experimental day. WR and CTRL-WR mice had free access to food and water at all times. On the day of termination, CTRL-WR mice were kept in home cages with locked running wheel for 2 h, while WR mice had their running wheel unlocked for 2 h. All mice were terminated immediately after end of exercise experiment. Running distance was measured by an odometer (Sigma Pure 1 Topline 2016, Sigma, Denmark). Wheel running habituation and exercise experiment were performed 1–3 h into the dark phase. After end exercise experiment, mice from WR group were divided into groups depending on running distance: Mice with running distance matching the treadmill running mice (WR_matched, 1.1< >1.6 km, n = 12), low runners (WR_low, distance <1.1 km, n = 5) and high runners (WR_high, distance >1.6 km, n = 8) (Fig. S1).

2.4. Plasma collection and analysis

On the day of termination, mice were anaesthetised by isoflurane/O_2 (Attane Vet., Scanvet animal Health, Fredensborg, Denmark) inhalation immediately after exercise exposure and blood was collected on wet-ice for plasma separation. Corticosterone was measured in mouse plasma using enzyme-linked immunosorbent assay (ELISA, Cat. No. 50-22-6, Biosite, Denmark). Fatty acids (FA) were measured in mouse plasma using NEFA-HR (2) Assay (FUJIFILM, Wako Chemicals, Europe) and triglycerides (TG) were measured in mouse plasma using Triglyceride LiquiColor® Test (Enzymatic) (Stanbio Laboratory, Cat. No. 2100-225, Block Scientific, Bellport, NY, USA). All assays were used according to the protocol provided by the manufacturer.

2.5. Tissue harvest and processing

Following blood collection, mice were perfused intracardially with heparinized PBS (15,000 IU/L) for 2 min and subsequently 10% neutral buffered formalin (NBF) (Sigma–Aldrich, Darmstadt, Germany) for 5 min. Brains were removed and post-fixed overnight in NBF at room temperature.

2.6. Whole-brain c-Fos staining and imaging

Brains were stained against c-Fos using previously described protocol for immunolabelling-enabled 3D imaging of solvent cleared organs (iDISCO) [29,31]. Antibodies included anti-c-Fos antibody (1:5000; 2250, Cell Signaling Technology, Danvers, MA, USA) and anti-Rb-Cy5 1:1000 (cat. No. 711-175-152, Jackson ImmunoResearch, West Grove, PA). Whole brains were imaged using a light sheet microscope (Miltenyi Biotec GmbH, Bergisch Gladbach, Germany) with Zyla 4.2PCL10 sCMOS camera (Andor Technology, Belfast, UK), MV PLAPO 2XC (Olympus, Tokyo, Japan) objective and SuperK EXTREME supercontinuum white-light laser EXR-15 (NKT Photonics, Birkerød, Denmark). Brains were imaged in axial orientation in a DBE filled chamber using two-sided illumination with an exposure time of

254 ms in a z-stack at 10 μm intervals at 0.63 × magnification (1.2 × total magnification). Data was acquired in two channels, autofluorescence at 560 ± 20 nm (excitation) and 650 ± 25 nm (emission) wavelength (80% laser power) and c-Fos staining at 630 ± 15 nm (excitation) and 680 ± 15 nm (emission) wavelength (100% laser power).

2.7. Semi-systematic literature review

To assess the extent of lacking proper controls in animal exercise studies using treadmills and running wheels, we conducted a review of published articles in five selected top-tier journals: Cell Metabolism, Nature Metabolism, Nature, Science, and Cell. Using the websites of these journals and the search terms "treadmill" and "wheel-running" were used and the searches were conducted in July and August of 2023.

The search using "Treadmill" as search term returned the following hits published within the period of January 2019 to June 2023: Nature Metabolism (24 hits, 14 relevant articles), Cell Metabolism (27 hits, 19 relevant articles), Cell (27 hits, 2 relevant articles), Nature (84 hits, 6 relevant articles), Science (31 hits, 7 relevant articles). The search using "Wheel-running" as search term returned the following hits within the period of January 2019 to June 2023: Nature Metabolism (13 hits, 9 relevant articles of which 6 articles were also identified in the "Treadmill" search), Cell Metabolism (38 hits, 10 relevant articles of which 4 articles were also identified in the "Treadmill" search), Cell (269 hits, 5 relevant articles of which 2 articles were also identified in the "Treadmill" search), Nature (7 hits, 4 relevant articles of which 1 articles were also identified in the "Treadmill" search), Science (73 hits, 3 relevant articles of which 2 articles were also identified in the "Treadmill" search). Hits considered "not relevant" were other types of articles than original research articles or not directly related to exercise biology in rodents. A list of all relevant articles can be found in Table S3. In this table, irrelevant hits are highlighted in grey. Studies that provide insufficient information on control-handling or state that controls are kept in home cage are highlighted in red, and studies reporting exposure of controls to either running wheel or treadmill are highlighted in green.

2.8. Image analysis

Image processing and quantification of c-Fos positive cells was performed according to previously described method [32]. Individual c-Fos segmentation volumes were generated and to enable region-wise quantification of c-Fos positive cells, the segmentation volumes were aligned to a digital LSFM-based mouse brain atlas [32], which is based on the common coordinate framework version 3 (CCFv3) developed by Allen Institute of Brain Science. The alignment was performed through an affine and a B-spline-based registration using the Elastix toolbox [33]. Density heatmaps, visualizing the density of c-Fos positive cells, were generated by aligning the cell-segmentation volumes to the LSFM atlas using an inverse transform followed by generating and summing up spheres of uniform value in a 100 μm radius around each detected c-Fos positive cell. Heatmaps depicting up- and downregulation of c-Fos expression were created by subtracting the group average control heatmap (n = 8 brains) from the group average heatmap (n = 8–12 brains) and removing signal from non-significant brain regions. Principal component analysis and hierarchical clustering were performed on relative mean c-Fos cell count, centered and scaled across all brain regions. Image analysis and processing were performed in Python and 3D brain visualizations were created using the ImarisTM software version 2 (Oxford instruments, Abington, UK).

2.9. Statistical analysis

Whole-brain c-Fos cell counts were analysed using both region-based and voxel-based statistics similar to what has been described previously [32]. Region-based analysis was performed on 438 atlas-defined brain regions. A generalised linear model (GLM) was fitted to the number of detected c-Fos positive cells in each brain region of every animal. For each GLM, a Dunnett's test was performed, and subsequently Benjamini-Hochberg false discovery (FDR) correction was applied to correct for multiple comparison ($p < 0.05$). Manual validation was conducted to verify that the datapoints follow the negative binomial distribution and significance of the regions were not achieved due to outliers. Deviance residuals were investigated, and significant regions were discarded if residuals violated the assumptions of normality and homoscedasticity. Moreover, Cook's distance was used to discard any significant regions with overly influential data points.

Voxel-based statistical analysis was performed on cell segmentation volumes converted to the LSFM-based mouse brain atlas space. At each voxel position, Welch's t-test was performed between groups, and the corresponding p-value was converted to a standard Z-score.

Plasma data and c-Fos counts in selected brain regions were analysed using two-way ANOVA with Tukey–Kramer post hoc test to account for unequal samples size when interactions between exercise and exercise modality was reported. Initial c-Fos quantification was performed on brains from all 49 animals. In second, and final iteration of the analysis, 13 mice with running distances <1.1 km (n = 5) and >1.5 km (n = 8) were removed from the study (Fig. S1, Table S1). Running distance and running time data were analysed using unpaired t-test. Whole-brain statistical analysis was performed using R packages MASS, multcomp, lmtest and car. Two-way ANOVA was performed using GraphPad Prism 9.0 (GraphPad, USA).

3. RESULTS

3.1. Acute exercise induces profound neuronal c-Fos activation

To understand how exercise impacts brain activity, we compared whole-brain activation profiles of mice exposed to treadmill running and mice exposed to distance-matched wheel running. Four groups of young adult male mice were subjected to either an acute bout of 2 h voluntary wheel running (WR, n = 25), 1-hour forced treadmill running until exhaustion (TR, n = 8), rest in either a cage with a locked running wheel (CTRL-WR, 2 h, n = 8) or on an inactive treadmill (CTRL-TR, 1 h, n = 8). Immediately following the intervention, blood was collected for plasma analysis and brains were collected for whole-brain c-Fos quantification (Figure 1A). Twelve mice from the voluntary wheel running paradigm, for which running time and distance closely matched the treadmill running group (Figure 1B–E), were selected for further analysis (Fig. S1). Light-sheet fluorescence microscopy (LSFM) was used to assess the whole-brain activation signature in response to exercise (Movie S1, S2, and Fig. S2). We observed an extensive brain-wide c-Fos upregulation in response to both forced treadmill running and voluntary wheel running, with much more wide-spread c-Fos upregulation detected in treadmill running group (Figure 1F–G). Strikingly, a pronounced c-Fos induction was not only observed in exercising mice, but also in control mice that were placed on an inactivated treadmill (CTRL-TR). In these mice, induction of c-Fos was induced more widespread and stronger than in mice in the wheel running group. In contrast, mice that were exposed to a locked running wheel in their home-cage displayed only a limited number of c-Fos positive cells (Figure 1H). Brain-wide total c-Fos positive cell count indicated a 3.6-times trend for an increase in therunning wheel group compared to mice housed with a locked running wheel (100 ± 34 ×

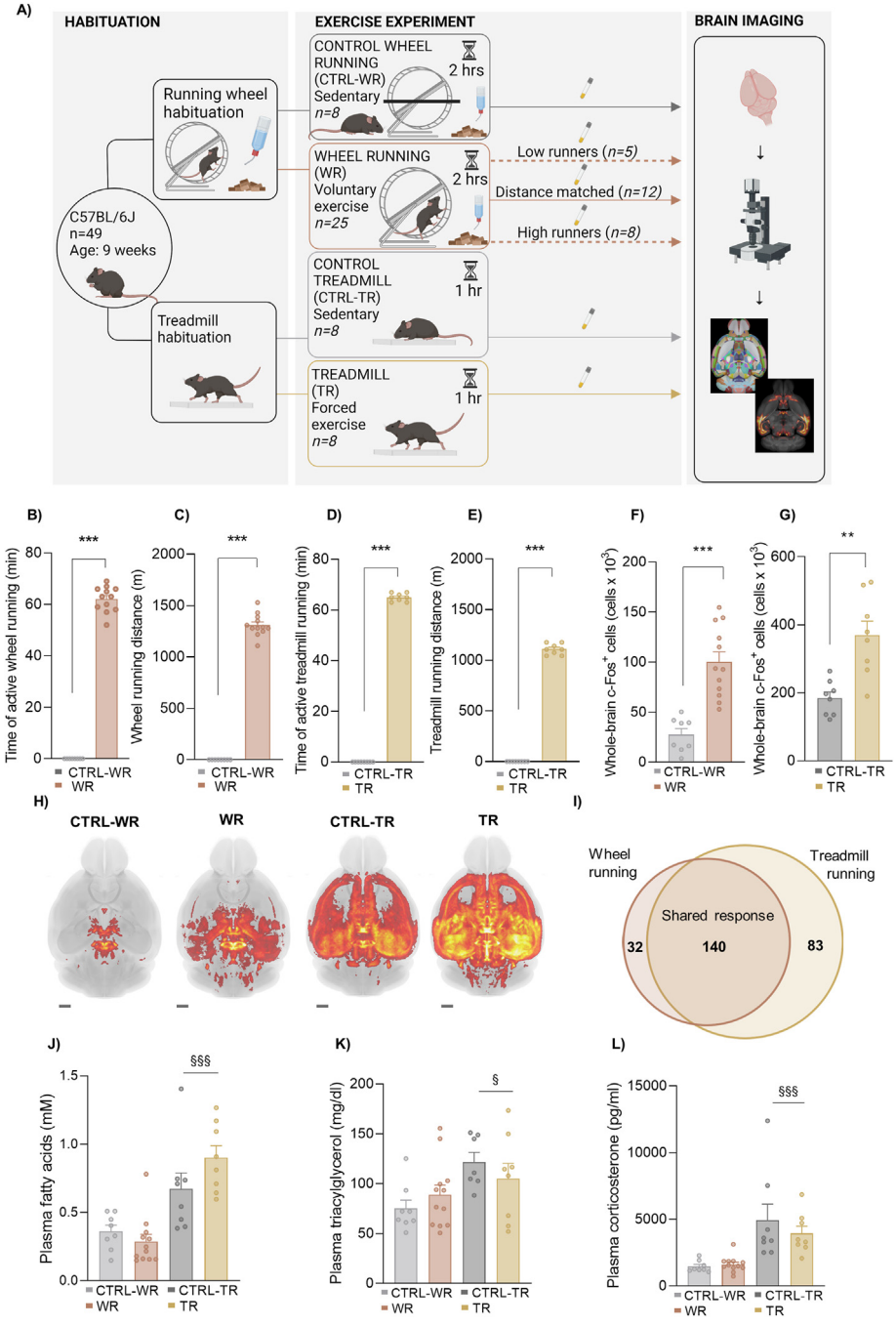

Figure 1: Exercise has pronounced effect on brain activity in mice (A) 49 young male C57Bl/6J mice were randomized to 2 h in home cage with inactive running wheel (CTRL-WR), 2 h in home cage with active running wheel (WR), 1 h rest on inactive treadmill (CTRL-TR), or 1 h forced treadmill exercise until exhaustion (TR). Brains were collected for whole-brain c-Fos quantification. (B) Time of active running wheel (min) for CTRL-WR and WR. Data were analysed using unpaired t-test ($^{***}p < 0.001$). (C) Running distance (m) of CTRL-WR and WR. Data were analysed using unpaired t-test ($^{***}p < 0.001$). (D) Time of active treadmill (min) CTRL-TR and TR. Data were analysed using unpaired t-test ($^{***}p < 0.001$). (E) Running distance (m) of CTRL-TR and TR. Data were analysed using unpaired t-test ($^{***}p < 0.001$). (F) Number of c-Fos positive cells (group average ± SEM) in the whole brain of WR and CTRL-WR. Data were analysed using unpaired t-test ($^{***}p < 0.001$). (G) Number of c-Fos positive cells (group average ± SEM) in the whole brain of TR and CTRL-TR. Data were analysed using unpaired t-test ($^{**}p < 0.01$). (H) Whole-brain heatmaps depicting average c-Fos signal in each group. (I) Proportional venn diagram illustrating the number of significant brain regions unique for TR when compared to CTRL-TR (83 regions, not regulated by WR), number of significant brain regions unique for WR when compared to CTRL-WR (32 regions, not regulated by TR), and number of significant regions shared among the two exercise paradigms (140 regions). (J) Plasma levels of fatty acids (mM) in each group (average ± SEM). Two-way ANOVA demonstrated main effect of exercise modality ($^{§§§}p < 0.001$; WR groups vs. TR groups). (K) Plasma levels of triacylglycerol (mg/dl) in each group (average ± SEM). Two-way ANOVA demonstrated main effect of exercise modality ($^{§}p < 0.05$; WR groups vs. TR groups). (L) Plasma levels of corticosterone (pg/ml) in each group (average ± SEM). Two-way ANOVA demonstrated main effect of exercise modality ($^{§§§}p < 0.001$; WR groups vs. TR groups). Scale bars: 1000 μm.

10^3 and 27 $\pm$ 16 $\times$ 10^3, p = 0.08, c-Fos positive cells on average, respectively). In contrast, because control mice on the inactivated treadmills displayed a profound induction of c-Fos, only a 2-fold increase in c-Fos positive cells was observed with treadmill running group compared to the control group (369 $\pm$ 111 $\times$ 10^3 and 185 $\pm$ 47 $\times$ $10^{3,}$ c-Fos positive cells on average, respectively) (Figure 1F, G). These data imply a higher sensitivity to wheel running relative to treadmill running for distinguishing exercise-induced neuronal activation. To further assess exercise-modality specific differences in brain activation, we quantified the number of c-Fos positive cells in 438 atlas-defined brain regions (Table S1 + Fig. S2). This revealed that 140 brain regions (55% of all regulated brain regions) were activated by both exercise interventions in comparison to the controls (Figure 1H, I). We also discovered that 83 brain regions were uniquely regulated by treadmill running and that 32 brain regions were uniquely regulated by wheel running (Figure 1I). Furthermore, analyses of the circulating levels of fatty acids (Figure 1J) and triacylglycerol (Figure 1K) unveiled an increase in these lipids simply by placing mice on the treadmills, irrespective of whether they were forced to run or not. This observation potentially corresponds to stress-triggered adipose tissue lipolysis and hepatic VLDL-TG release. In alignment with this interpretation, mice subjected to both treadmill running and treadmill control conditions demonstrated similarly elevated plasma corticosterone levels (Figure 1L), reinforcing the association with stress-induced responses. Previous reports on corticosterone levels in response to light exercise have been variable [34], probably due to discrepancies in study designs, as corticosterone fluctuate with the time of the day. However, in agreement with previous findings [20], treadmill exercise induced a marked increase in corticosterone levels. Supplementary video related to this article can be found at https://doi.org/10.1016/j.molmet.2024.101907

3.2. Common and unique neuronal activation signatures of forced treadmill running and voluntary wheel running

To further elucidate differences in c-Fos upregulation in response to treadmill running and wheel running (Figure 2A), we conducted a hierarchical clustering analysis (Figure 2B, C). The principal component analysis (PCA) demonstrated clustering of samples based on their c-Fos activation signatures (Figure 2B) and the subsequent clustering analysis emphasized the increase in c-Fos positive cells in multiple brain regions in mice exposed to treadmill running (Figure 2C, Table S2). The analysis further revealed that most brain regions demonstrated higher c-Fos cell count in treadmill running group than in the wheel running group and only a few brain regions demonstrated higher c-Fos positive cell count in wheel running group compared to treadmill running (Figure 2C). Moreover, cluster 4 characterized by a high number of c-Fos positive cells in the treadmill running group, demonstrated an overlap of c-Fos activity between the treadmill running group and its control, whereas more separation was observed between wheel running group and its control in cluster 2.

With the aim of characterizing the brain activity profiles of forced treadmill running and voluntary wheel running, we used the Allen Brain Atlas anatomical hierarchy to generate a complete list of brain regions significantly regulated by each exercise paradigm (Fig. S3 and Fig. S4). Notably, brain regions activated by both exercise paradigms (shared response) were found to be predominantly located within isocortical regions, e.g., primary motor area (MOp), retrosplenial areas (RSP) and the hippocampal formation (e.g., dentate gyrus (DG) and Cornu Ammonis (CA) areas). These brain regions have all previously been linked to exercise [35,36]. However, also brain regions that have not previously been associated with exercise emerged from the analysis as part of the shared response to forced treadmill and voluntary wheel running. This included brain regions within the cortical subplate, such as the thalamus, pons, and the medulla (Figure S3,S4). The number of brain regions uniquely regulated by voluntary wheel running were limited but were also mostly regions not previously linked to exercise and were located in different anatomical regions, such as the hypothalamus, cerebellum, and medulla. Remarkably, brain regions uniquely regulated by forced treadmill running were primarily located in the hypothalamus and striatum, with the majority of regions being part of the limbic pathway. This probably reflect stress and fear, evidenced by regulation of the central amygdala (CEA) [37], the anterior cingulate area (ACA) [38], and the ventromedial hypothalamic nucleus (VMH) [39].

3.3. Voluntary wheel running display a unique brain activity signature

Following the discovery that forced treadmill exercise and voluntary wheel running give rise to distinct c-Fos activation signatures, we sought to scrutinize the brain signatures in further detail aiming to unveil novel exercise-induced neurobiological insights. To accommodate this, we applied two different statistical analyses (Fig. S2). First, voxel-based statistical analysis was applied to average c-Fos heatmaps [32], depicting all voxels with statistically significant average c-Fos signal in wheel running group when compared to its control group ($p < 0.05$, Figure 3A). This was used as a visual aid to support conclusions from the region-based analysis. The region-based statistical analysis was performed to report all brain regions with a statistically different number of c-Fos positive cells in the wheel running group compared to its control (Figure 3B). A significantly increased number of c-Fos positive cells was found in a total of 172 brain regions in wheel running group when compared to its control (Figure 3B). No brain regions demonstrated a significant decrease in c-Fos positive cells (Figure 3B). Out of the 172 significantly upregulated brain regions, 32 regions were uniquely regulated by voluntary wheel running, i.e. were not significantly regulated by treadmill running when compared to their respective control groups (Figure 3C). Given the high c-Fos level in treadmill controls, we hypothesized that most of these unique wheel running regions were also activated by treadmill running, but not statistically significant, due to control-subtraction. Hence, we compared the number of c-Fos positive cells in the two runners groups without control-subtraction to elucidate any regions statistically significant between wheel running and treadmill running, irrespective of c-Fos levels in controls.

Using this strategy, we demonstrated significantly increased c-Fos activity in 4 brain regions from the voluntary wheel running group compared to the treadmill running group (the dentate nucleus, DN; the medullary reticular nucleus, ventral part, MDRNv; the nucleus prepositus, PRP; and the fields of forel, FF) (Figure 3C, D). In line with previous findings, we observed activation of subnuclei within the ventral part of the DN, a deep cerebellar region, involved in limb movement [40] (Figure 3E—H). Through striatal interactions, the DN is reported to participate in reward signalling and could be involved in the motivational aspects of voluntary running [41,42]. Another region that demonstrated increased c-Fos expression following wheel running when compared to treadmill running was the fields of forel (FF) (Figure 3I-L), a brain region consisting of dense nerve bundles projecting from the thalamus to the globus pallidum and cerebellum, and that has reported to be involved in involuntary movement [43]. Other regions uniquely activated by voluntary wheel running included

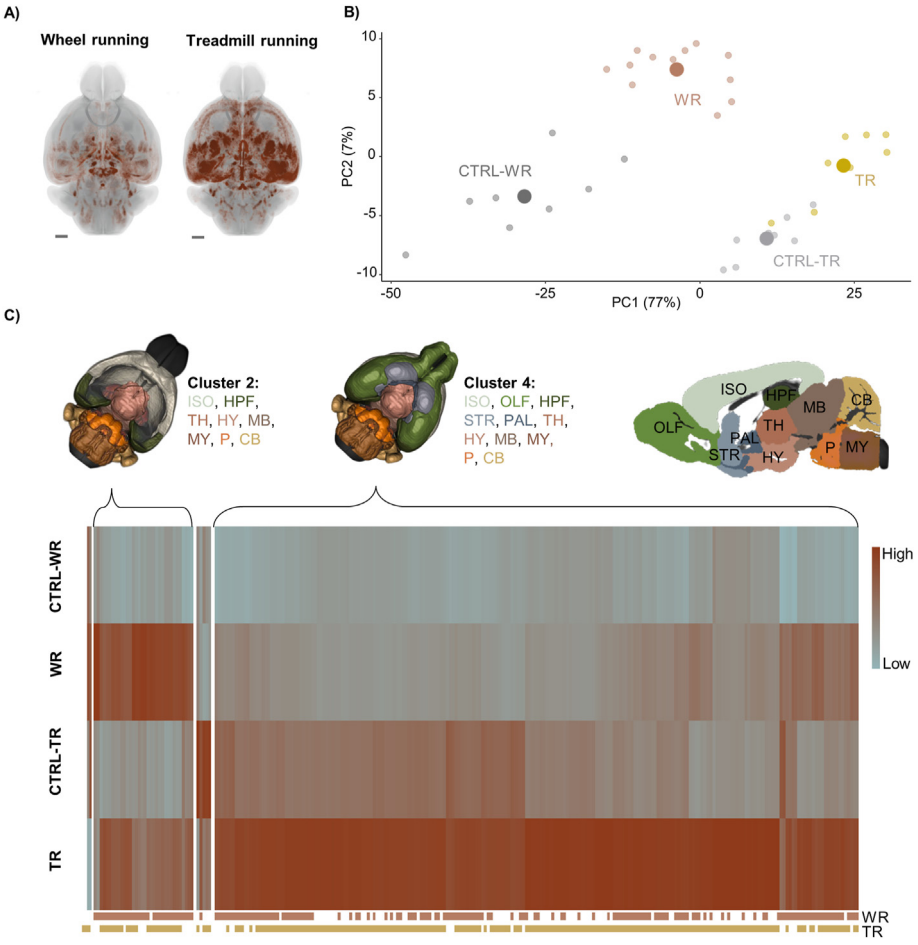

Figure 2: Voluntary wheel running and forced treadmill running elicit distinct brain activation signatures (A) Heatmaps (dorsal view) depict control-subtracted average whole-brain c-Fos expression responses to forced treadmill running or voluntary wheel running (n = 8–12 mice per group). Voxels with increased average c-Fos count (in WR compared to CTRL-WR; TR compared to CTRL-TR) are depicted in red and voxels with reduced average c-Fos count are depicted in blue (none). Scale bars: 1000 μm. (B) Principal component analysis (PCA) plot illustrating distinctness in region-based c-Fos counts between samples defined by the first two principal components, PC1 and PC2, accounting for most variance in the data are shown. (C) Heatmap depicting relative mean c-Fos count within each brain region of each group (scalebar: low to high), divided into 4 clusters. Major brain divisions activated in the two main clusters, cluster 2 and 4, are depicted as 3D volumes and sagittal section using Allen Brain Atlas nomenclature. Minor cluster 1 consists of two brain regions that are low in treadmill running group. These brain regions are Interstitial nucleus of Cajal and the Intergeniculate leaflet of the lateral geniculate complex, that both receive retinal input for oculomotor control and circadian rhythmicity, respectively. Minor cluster 3 is characterized by brain regions with a high number of c-Fos positive cells in the CTRL-TR group. This includes different parts of the interpeduncular nucleus, the lateral habenula as well as the posterior part of the cortical amygdala (for details, see Table S2). Lines below heatmap depict brain regions with statistically significantly different number of c-Fos positive cells in WR compared to CTRL-WR (red) and TR compared to CTRL-TR (yellow). Data was analysed using Dunnett's test negative binomial generalised linear model and FDR <0.05 for p-value adjustment. Abbreviations: cerebellum (CB), hippocampal formation (HPF), hypothalamus (HY), isocortex (ISO), midbrain (MB), medulla (MY), olfactory areas (OLF), pallidum (PAL), pons (P), striatum (STR), thalamus (TH).

the nucleus prepositus (PRP) that plays a role in eye movements during changes in head posture [44] and thus might be activated when mice run in the rotating running wheel. Moreover, the ventral part of the medullary reticular nucleus (MDRNv) was also found to be activated specifically by wheel running (Fig. S5). The role of this region in wheel running is unclear but might be worth noticing that the lateral part has been suggested to control cardiovascular and respiratory functions [45] (Fig. S5). Regarding the potential physiological function of these brain regions, it is interesting to note that activation in response to wheel running seems to be unrelated to the total running distance, as illustrated by data obtained in MDRNv (Fig. S5D) and PRP (Fig. S5H) but also DN and FF (Fig. S5). This might suggest that activation of these regions reflect neurological responses that are related to altered housing enrichment rather than a response to the exercise stimuli *per se*.

3.4. Forced treadmill running activates brain regions involved in stress and nociception

After assessing the unique brain activation profile in response to voluntary wheel running, we examined the activation signature induced by forced treadmill running. A voxel-based statistical map depicted all voxels with statistically significant average c-Fos signal in the treadmill running group compared to its control demonstrating that despite high levels of c-Fos in the treadmill control group, significant differences were observed throughout the brain (Figure 4A). The subsequent regional analysis demonstrated a total of 223 brain regions significantly regulated by forced treadmill running, out of which 6 regions were downregulated (Figure 4B). While 83 out of the 223 regions were uniquely regulated by treadmill running, it could be that several of these regions were activated as a part of a broader stress response rather than being specific to the treadmill running *per se* [18]. The pronounced

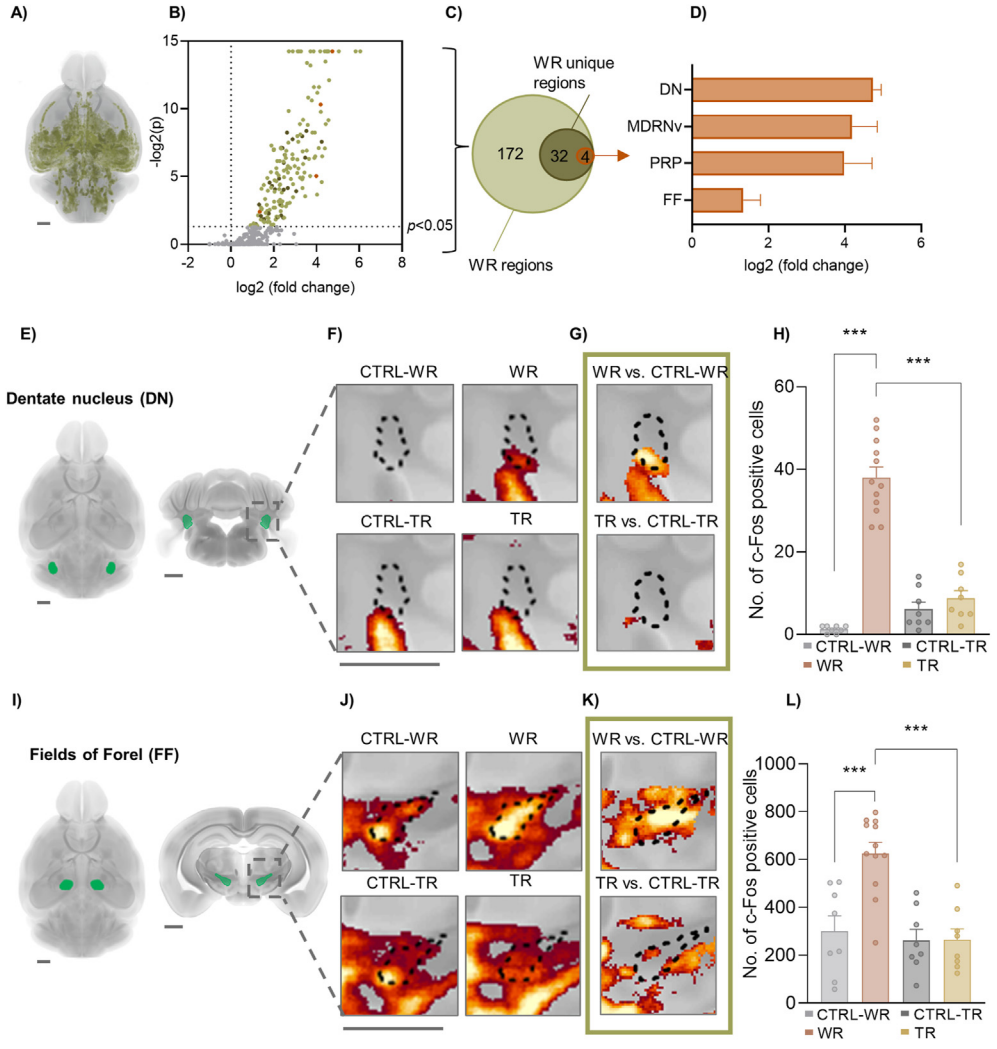

Figure 3: Selected brain regions activated by voluntary wheel exercise (A) Whole-brain voxel-wise Z-score map illustrates statistically significant ($p < 0.05$; Welch's t-test) brain activity in wheel running mice compared to wheel running controls, dorsal view. (B) Volcano plot showing all brain regions with regulation of c-Fos cell count in WR mice compared to CTRL-WR. Colours indicate brain regions with upregulation of c-Fos protein (light green, n = 172 regions) by WR, brain regions regulated by wheel running exclusively, i.e. not regulated by treadmill running (dark green, n = 32 regions) and brain regions with increased c-Fos when compared to TR (orange, n = 4 regions). Statistically insignificant brain regions are reported in grey ($p > 0.05$). Dotted vertical line indicates fold change 0 and horizontal line indicates threshold for p value ($p < 0.05$; Dunnett's test negative binomial generalised linear model and FDR <0.05 for p-value adjustment. (C) Proportional Venn diagram illustrating number of brain regions significantly regulated by WR, WR unique regions and regions upregulated compared to TR. (D) Unique WR brain regions upregulated when compared to TR, ranked by significance ($p < 0.05$). (E + I) 3D reconstructed average mouse brain (dorsal view) with delineation of Fields of Forel or Dentate nucleus (DN) in green (left) and virtual coronal section delineating the brain region in green (right). (F + J) Heatmaps (virtual coronal sections) depict average whole-brain c-Fos expression within the FF or DN of brains from each group (n = 8–12 mice per group). (G + K) Virtual coronal sections of the voxel-wise Z-score map illustrates statistically significant voxels within the FF or DN for the individual exercise modality when compared to its control. Threshold: p = 0.05; Welch's t-test. (H + L) Number of c-Fos positive cells in the FF or DN of each group. Data was analysed with two-way ANOVA followed by Tukey–Kramer multiple comparison test, $***p < 0.001$. Scale bars: 1000 μm.

c-Fos staining throughout the brain in the treadmill control group combined with high corticosterone levels in plasma, implies that placing mice on an enclosed treadmill for ~60 min is a severe stressor. Consequently, we decided to compare the number of c-Fos positive cells in treadmill control group (CTRL-TR) with the wheel running control group (CTRL-WR) and subsequently subtracted all regions that were significantly different between controls from the TR response. This resulted in 30 regions that were found to be the specifically induced by treadmill running (Figure 4C, D). Within these 30 treadmill running-regulated regions, we found nucleus raphe magnus (RM, Figure 4E–H), a brain region extensively studied for its role in pain modulation [46]. Since neuronal pathways for pain and stress are interconnected [47], we decided to delve deeper into the 83 brain regions regulated by forced treadmill running and found several brain regions involved in the ascending and descending pathways of nociception (Figure 4I) [48–51]. Electrical shock for running motivation was part of the treadmill running protocol, and this could be the explanation for activation of the ascending pain pathway. However, the descending pain pathway, responsible for pain modulation, mediated by locus coeruleus (LC) and RM via nociceptive input from the periaqueductal gray (PAG) [52], may be activated due to a general stress response stimulated by the hypothalamic–pituitary–adrenal (HPA) axis [47].

3.5. Common exercise-induced neuronal activation signature

Following the mapping of unique activation signatures of each exercise intervention, we went on to characterize the shared exercise

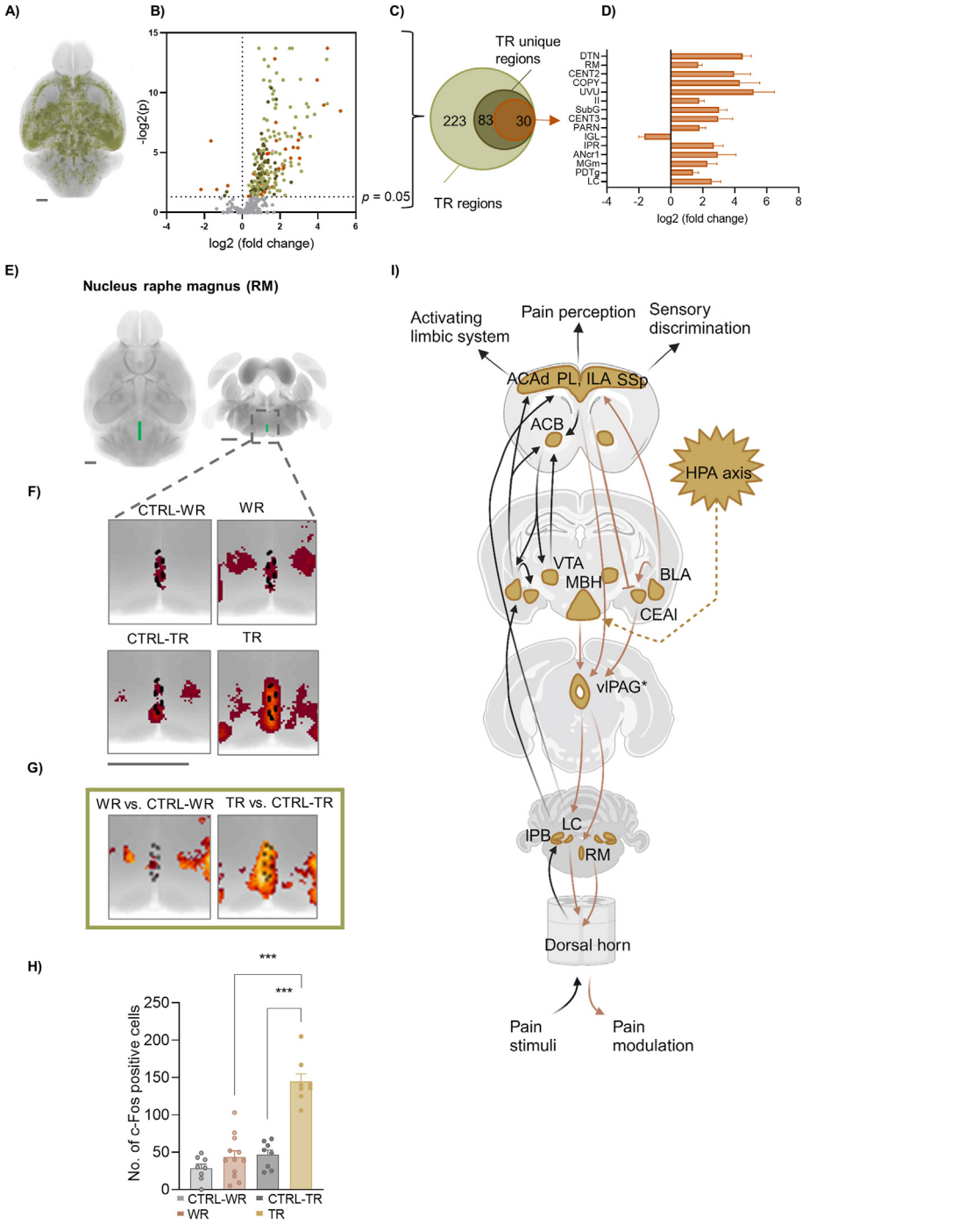

Figure 4: Selected brain regions activated by forced treadmill running (A) Whole-brain voxel-wise Z-score map illustrates statistically significant ($p < 0.05$; Welch's t-test) brain activity in treadmill running (TR) mice compared to treadmill controls (CTRL-TR), dorsal view. (B) Volcano plot showing all brain regions with regulation of c-Fos expression in TR mice compared to CTRL-WR. Colours indicate brain regions with regulation of c-Fos protein (light green, n = 223 regions) by TR, brain regions regulated by TR exclusively, i.e. not regulated by WR (dark green, n = 83 regions) and unique TR regions that are not upregulated by CTRL-TR when compared to CTRL-WR, i.e. not regulated by stress (orange, n = 30 regions). Statistically insignificant brain regions are reported in grey ($p > 0.05$). Vertical line indicates fold change 0 and dotted horizontal line indicates threshold for p value ($p < 0.05$; Dunnett's test negative binomial generalised linear model and FDR <0.05 for p-value adjustment). (C) Proportional Venn diagram illustrating number of brain regions regulated by TR, TR unique regions and TR regions not regulated by stress. (D) Unique TR brain regions not regulated by stress, ranked by significance ($p < 0.05$). (E) 3D reconstructed average mouse brain (dorsal view) with delineation of Nucleus raphe magnus (RM) in green (left) and virtual coronal section delineating the brain region in green (right). (F) Heatmaps (virtual coronal sections) depict average whole-brain c-Fos expression within the RM of brains from each group (n = 8–12 mice per group). (G) Virtual coronal sections of the voxel-wise Z-score map illustrates statistically significant voxels within the RM for the individual exercise modality when compared to its control. Threshold: p = 0.05; Welch's t-test. H) Number of c-Fos positive cells in the RM of each group (average ± SEM). Data was analysed with two-way ANOVA followed by Tukey–Kramer multiple comparison test, ***$p < 0.001$. I) Brain regions significantly regulated by treadmill running involved in pain facilitation and modulation. www.neuropedia.dk Abbreviations: Anterior cingulate area, dorsal part (ACAd), nucleus accumbens (ACB), basolateral amygdala (BLA), central amygdalar nucleus, lateral part (CEAl), infralimbic area (ILA), locus ceruleus (LC), mediobasal hypothalamus (MBH), periaqueductal gray, ventrolateral part (vlPAG), prelimbic area (PL), primary somatosensory area (SSp), nucleus raphe magnus (RM), parabrachial nulcues, lateral part (lPB), ventral tegmental area (VTA). Scale bars: 1000 μm *PAG is not statistically significant in TR compared to CTRL-TR, but increased in both groups.

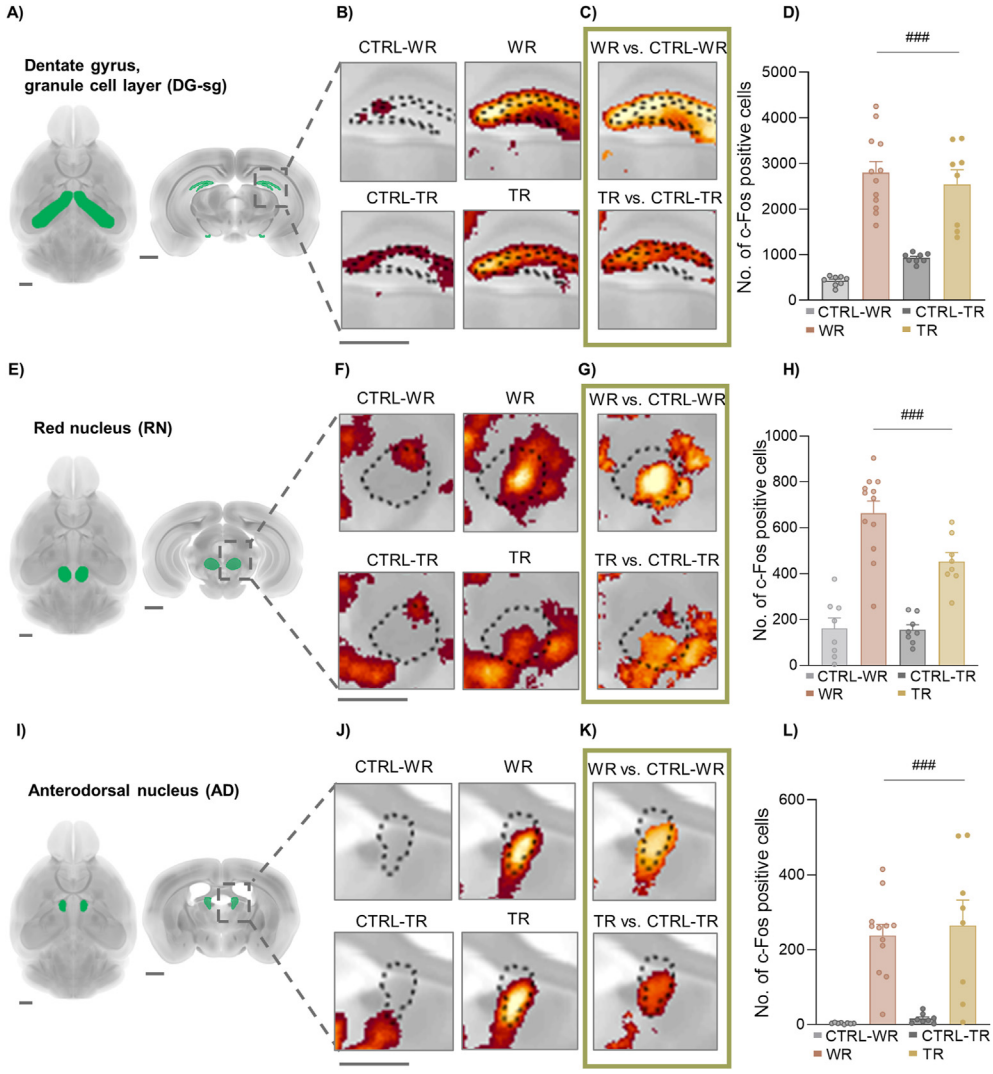

Figure 5: Selected brain regions regulated by both exercise paradigms (A + E + I) 3D reconstructed average mouse brain (dorsal view) with delineation of Dentate gyrus, granule cell layer (DG-sg), Red nucleus (RN), or Anterodorsal nucleus (AD) in green (left) and virtual coronal section delineating the brain region in green (right). (B + F + J) Heatmaps (virtual coronal sections) depict average whole-brain c-Fos expression within the DG-sg, RN or AD of brains from each group (n = 8–12 mice per group). (C + G + K) Virtual coronal sections of the voxel-wise Z-score map illustrates statistically significant voxels within the DG-sg, RN or AD for the individual exercise modality when compared to its control. Threshold: p = 0.05; Welch's t-test. (D + H + L) Number of c-Fos positive cells in the DG-sg, RN or AD of each group (average ± SEM). Data was analysed with two-way ANOVA. Main effect of exercise: $^{###}p < 0.001$. Scale bars: 1000 μm.

brain activation response. Out of the 140 brain regions with increased c-Fos expression in response to both forced treadmill running and voluntary wheel running, we noted several previously identified exercise-related brain regions, for example the dentate gyrus (Figure 5A–D) [35]. We also observed increased c-Fos activation within the red nucleus (RN) following both exercise interventions, with a tendency for higher c-Fos activation in wheel running mice compared to treadmill running mice (Figure 5E–H). RN is mostly acknowledged for its role in motor control [53], but has more recently been implicated in exercise reinforcement through its projections to the ventral tegmental area (VTA) [9]. Notably, we also identified several new exercise-related brain regions that were part of the shared response. One example is the anterodorsal nucleus (AD) for which a prominent c-Fos induction was found following both wheel running and treadmill running (Figure 5I-L). This brain region plays a significant role in spatial learning, memory, and attention [54].

3.6. Treadmill exposure triggers a pronounced stress response in the brain

Our observations are consistent with the literature that suggests that forced treadmill running is stressful [18,19]. Furthermore, the widespread c-Fos induction observed in non-running mice positioned on an idle treadmill (Figure 6A, B) indicates that the significant level of stress arises not solely from treadmill running but is contributed by preconditioned association of the treadmill with stress. To assess the contributing from and confounding effects of the control groups to the neuronal activity signatures, we generated a whole-brain heatmap demonstrating extensive brain-wide c-Fos upregulation in the treadmill control group compared to running wheel control (Figure 6C). The subsequent region-based analysis demonstrated 211 significantly upregulated brain regions in the treadmill control group compared to the wheel running control (Figure 6D). These regions included the periaqueductal gray (PAG), specifically the dorso-medial (dm) and

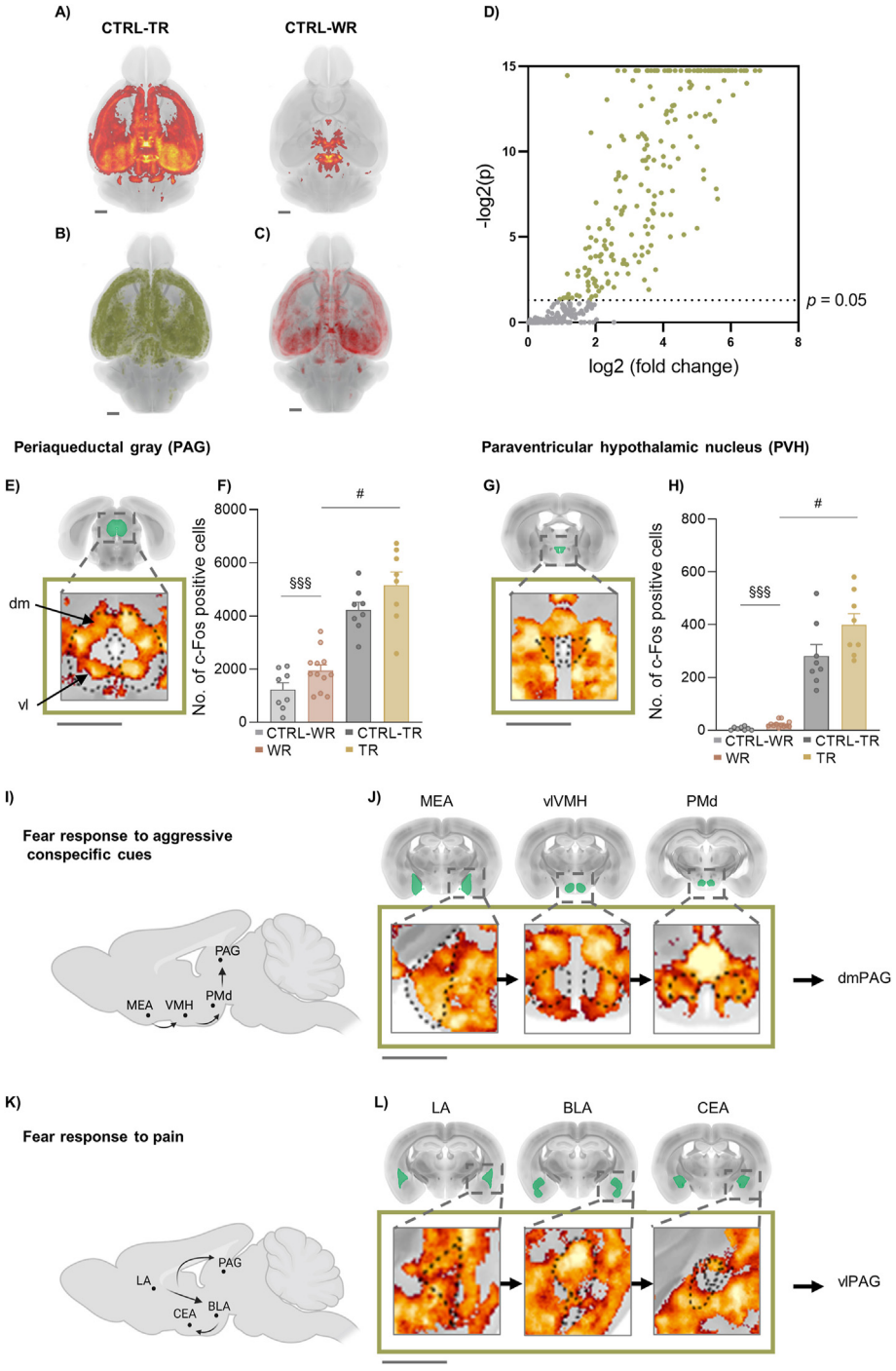

Figure 6: Stress - and fear-induced c-Fos activation in treadmill control mice (A) Whole-brain heatmaps depicting average c-Fos expression in treadmill control (CTRL-TR) and voluntary running control (CTRL-WR) groups. (B) Whole-brain voxel-wise Z-score map illustrates statistically significant ($p < 0.05$; Welch's t-test) brain activity in CTRL-TR mice compared to CTRL-WR, dorsal view. (C) Heatmap (dorsal view) depict CTRL-WR-subtracted average whole-brain c-Fos expression (n = 8) in CTRL-TR. Voxels with increased average c-Fos signal depicted in red and brain areas with reduced average c-Fos signal are depicted in blue (none). (D) Volcano plot depicting all brain regions with regulation of c-Fos expression in CTRL-TR mice compared to CTRL-WR. Light green colour indicates brain regions with upregulation of c-Fos protein (n = 210 regions) in CTRL-TR compared to CTRL-WR. Statistically insignificant brain regions are reported in grey ($p > 0.05$). Dotted horizontal line indicates threshold for p value ($p < 0.05$; Dunnett's test negative binomial generalised linear model and FDR <0.05 for p-value adjustment). (E + G) Virtual coronal section showing statistically significant voxels ($p < 0.05$; Welch's t-test) in periaqueductal gray (PAG) and paraventricular hypothalamic nucleus (PVH). (F + H) Number of c-Fos positive cells in the PAG and PVH of each group. Data was analysed with two-way ANOVA. Main effect of exercise: $^{\#}p < 0.05$ and main effect of exercise modality: $^{§§§}p < 0.001$, WR groups vs. TR groups. (I + K) Illustration of pathway for fear to aggressive conspecific cues leading to activation of the dorsomedial (dm) PAG and pathway for fear to pain leading to activation of the ventrolateral (vl) PAG. (J + L) Virtual coronal sections showing statistically significant voxels ($p < 0.05$; Welch's t-test) in medial amygdalar nucleus (MEA), ventromedial hypothalamic nucleus (VMH), dorsal premammillary nucleus (PMd), lateral amygdalar nucleus (LA), basolateral amygdalar nucleus (BLA), and central amygdalar nucleus (CEA). Scale bars: 1000 μm.

ventro-lateral (vl) segments of PAG were enriched for c-Fos in treadmill control mice compared to running wheel controls (Figure 6E, F). These subregions of PAG are linked to fear responses and learned fear retrieval [35,39,41]. In line with this, the paraventricular hypothalamic nucleus (PVH), was strongly activated by treadmill exposure (Figure 6G, H), indicative of HPA axis activation [55,56] and thus consistent with the increased plasma corticosterone levels observed in these groups. We also found brain regions activated downstream of the dmPAG, such as the medial amygdalar nucleus (MEA), ventro-lateral divisions of the ventromedial hypothalamic nucleus (vlVMH) and dorsal premammillary nucleus (PMd) (Figure 6I, J), corresponding to learned fear response to aggressive conspecific cues [39]. This fear pathway is activated upon olfactory input and thus possibly activated due to exposure of different mice to the same treadmill system with 4 parallel lanes. We also observed activation of lateral amygdalar nucleus (LA), basolateral amygdalar nucleus (BLA), and central amygdalar nucleus (CEA) which are upstream brain regions to vlPAG and implicated in the learned fear response to pain (Figure 6K, 6L). While the treadmill control mice were unlikely to get electrical shock on the experimental day (i.e., the treadmill was not active), they had been habituated similarly to the treadmill running group and for the habituation would have been exposed to the risk of electrical shock for motivation. Accordingly, they might associate the treadmill with painful stimuli, and thus display activation of a conditioned fear response to pain.

4. DISCUSSION

Amid a growing emphasis on the mental and cognitive benefits of exercise, there has been a notable surge in studies utilizing voluntary wheel running and forced treadmill running in rodents to investigate the mechanisms by which exercise affects the brain [57]. Strikingly, treadmill running and wheel running are often used interchangeably in the literature, and there have been little prior efforts to determine which intervention holds the highest predictive value for comprehending the neural benefits of exercise in humans. To date, most research into the neurological response triggered by exercise has relied on histological examination of predetermined brain regions. No prior studies have explored the global brain activation response to exercise. Here, we used a fully automated 3D quantitative imaging approach to map whole-brain activation signatures in response to forced treadmill running and voluntary wheel running in male mice. The extensive dataset generated by this study is available online at www.neuropedia.dk and we hope that this resource will support future research efforts in the field of exercise neurobiology.

One of the most notable findings of the present work is the overwhelming brain-wide neurological activation following both acute treadmill running and wheel running in mice. We found 140 brain regions regulated by both wheel running and treadmill running, independent of intervention type. This included several canonical exercise-related brain regions within hippocampal and cortical areas that are well-described in the context of long-term exercise [6]. We also identified significant activation of 89 brain regions beyond the hippocampus and the isocortex. It remains to be elucidated whether these acute effects observed in this study mirror initial neuronal alterations that contribute to the positive outcomes seen with chronic endurance exercise training. Notably, most of these regions have not previously been linked to exercise biology, underscoring an opportunity for future interventions to further elucidate the impact of exercise on the brain.

In addition to mapping the common neuronal responses between wheel and treadmill running, our results outlined substantial differences in brain activation signatures between these two exercise interventions. Accordingly, 83 brain regions were uniquely regulated by forced treadmill running and 32 brain regions were uniquely regulated by voluntary running. Intriguingly, the red nucleus was upregulated in both exercise models, with a tendency to be more increased in the group of wheel running mice than in the treadmill running mice. Interestingly, this brain region has recently been linked to exercise reward [9], thus not only supporting the widespread notion that exercise is a highly rewarding and reinforcing activity in mice [21], but also indicating that the rewarding effects might not be dependent on whether exercise is forced or voluntary [58]. However, to our surprise, regions of the mesocorticolimbic circuitry that generally play a significant role in motivation, such as ventral tegmental area (VTA) and nucleus accumbens (ACB), were activated by forced treadmill running, but not by voluntary wheel running. It should be noted that the VTA-ACB axis is also implicated in pain modulation [59,60]. Moreover, free access to running wheels may be suboptimal for assessing exercise motivation [61]. One study found that unexpected blocking of wheels following prolonged access elicited an activation of the striatum, prefrontal cortex, and lateral hypothalamus [61] and future studies with temporal c-Fos responses to different exercise paradigms are needed for additional insights into the rewarding aspects of running in mice. Finally, we discovered that voluntary wheel-running induced activity in hitherto novel brain regions in the context of exercise, such as the fields of forel (FF) and dentate nucleus (DN). It would be exciting for future studies to investigate the potential functional implication of these brain regions in the context of voluntary running.

In addition to the mesolimbic reward pathway, forced treadmill exercise also resulted in significant c-Fos induction in limbic-related regions associated with fear and stress responses [62,63], as well as regions linked to pain [46]. This 'adverse' neuronal profile coincided with high plasma levels of corticosterone that was evident in both treadmill runners and in treadmill control mice. The physiological significance of simply placing treadmill habituated mice on the treadmills, was underscored by the increased lipid and corticosterone levels and the remarkable 211 brain regions that displayed increased number of c-Fos positive cells in brains from treadmill control mice compared to brains from wheel running control mice. Several of the regions that were affected by changing the environment of the control animals are linked to fear and stress [62,63], implying how seemingly subtle differences in study design can heavily confound the outcome of brain-focused exercise studies. This challenge is likely not unique to the study of the neural response to exercise but might also confound the study of peripheral exercise responses, including signalling molecules secreted from various tissues and cell types during and after exercise. To explore if the absence of appropriate control groups in rodent exercise studies is a pervasive and wide-ranging issue, we reviewed the exercise-related papers that were published in five top-tier journals within the last 4 years. This indicated that treadmill running is a commonly employed methodology for studying exercise in rodents (Fig. S7A, Table S3). Of note, 88% of the identified treadmill studies that compared a group of 'exercised' mice with a group of 'non-exercised' control mice did either not expose control mice to an inactivate treadmill or did not sufficiently describe how sedentary controls were treated (e.g. if control mice were kept in their home cage or placed on an inactivate treadmill). Similarly, 84% of the identified wheel-running studies that compared a group of 'exercised' mice with a group of 'sedentary' control mice did either not expose control mice to a locked running wheel or did not sufficiently describe how sedentary controls were treated (e.g. if control mice had a locked running wheel placed in their home cage or not). Without subjecting sedentary control mice to an equivalent cage enrichment, such as one

with a locked running wheel, or specifically ensuring that they undergo identical handling procedures and stimuli as those in treadmill studies (excluding the running), there is a risk of drawing erroneous conclusions. Accordingly, attributing various biological effects solely to exercise may overlook potential confounding influences from other stressors or experimental procedure disparities.

In summary, we have created a comprehensive atlas of exercise induced brain activation and made this available as an online resource. Our results reveal a considerable overlap in neuronal activation signatures between voluntary wheel running and distance-matched forced treadmill running, but also bring to light significant differences and subtle nuances between these two widely used paradigms. Of particular significance, forced treadmill running triggers a peripheral stress response and activates brain regions associated with stress, pain, and fear. This raises concerns regarding the current utilization of forced treadmill running in rodent studies and calls into question the applicability of this specific intervention for investigating the neurobiological benefits of exercise in humans.

4.1. Limitations of the study

Whereas our study offers a comprehensive neurobiological snapshot of exercise-induced c-Fos activity, it offers no insights into the temporal changes that are likely to emerge in response to more prolonged exercise training interventions. Accordingly, it might be that the pervasive stress response to acute treadmill exercise will diminish over time with prolonged and repeated exposure. Moreover, it should be noted that using c-Fos as a proxy for neuronal activation provides no information on the targets of activation and further experiments should be conducted to elucidate neuronal circuits activated. Also, the quantification of c-Fos cells employs an in-house algorithm constructed to detect distinct c-Fos cell labelling in whole-mount cleared brains. In this study, we employ c-Fos as a surrogate marker for neuronal activity. While c-Fos is one of several early activation markers, examining others such as FosB and pCREB may uncover additional insights into the neurobiology of exercise.

CREDIT AUTHORSHIP CONTRIBUTION STATEMENT

Grethe Skovbjerg: Data curation, Formal analysis, Investigation, Methodology, Visualization, Writing — original draft, Writing — review & editing. **Andreas Mæchel Fritzen:** Investigation, Methodology, Writing — review & editing. **Charlotte Sashi Aier Svendsen:** Investigation, Methodology, Writing — review & editing. **Johanna Perens:** Investigation, Methodology, Writing — review & editing. **Jacob Lercke Skytte:** Investigation, Methodology, Writing — review & editing. **Camilla Lund:** Investigation, Methodology, Writing — review & editing. **Jens Lund:** Investigation, Methodology, Writing — review & editing. **Martin Rønn Madsen:** Investigation, Methodology, Writing — review & editing. **Urmas Roostalu:** Conceptualization, Methodology, Software, Supervision, Writing — review & editing. **Jacob Hecksher-Sørensen:** Conceptualization, Funding acquisition, Methodology, Project administration, Resources, Software, Supervision, Visualization, Writing — review & editing. **Christoffer Clemmensen:** Conceptualization, Funding acquisition, Project administration, Supervision, Visualization, Writing — original draft, Writing — review & editing.

ACKNOWLEDGEMENTS

We thank Thomas Topilko and Anders Bue Klein for helpful scientific discussions. G.S. receives funding from the Innovation Fund (grant number 9065-00237 B). C.C. receives funding from the Novo Nordisk Foundation Center for Basic Metabolic Research, an independent Research Center partially funded by an unconditionally donation from the Novo Nordisk Foundation (grant number NNF18CC0034900). A.M.F. is funded by the Novo Nordisk Foundation (grant number NNF 220C0074110). Figure 1A was created using BioRender.com.

DECLARATION OF COMPETING INTEREST

C.C. is co-founder of Ousia Pharma ApS. G.S, U.R., J.H-S., J.L.S. and J.P. are employed by Gubra.

DATA AVAILABILITY

Data are shared in the supplemental material and have been deposited on a publicly available webpage.

APPENDIX A. SUPPLEMENTARY DATA

Supplementary data to this article can be found online at https://doi.org/10.1016/j.molmet.2024.101907.

REFERENCES

[1] Mahalakshmi B, Maurya N, Da Lee S, Kumar VB. Possible neuroprotective mechanisms of physical exercise in neurodegeneration. Int J Mol Sci Aug. 2020;21(16):1—17. https://doi.org/10.3390/ijms21165895.

[2] Guo Y, Wang S, Chao X, Li D, Wang Y, Guo Q, et al. Multi-omics studies reveal ameliorating effects of physical exercise on neurodegenerative diseases. Front Aging Neurosci Oct. 31, 2022;14. https://doi.org/10.3389/fnagi.2022.1026688. Frontiers Media S.A.

[3] Liu Y, Yan T, Chu J, Chen Y, Dunnett S, Ho Y, et al. The beneficial effects of physical exercise in the brain and related pathophysiological mechanisms in neurodegenerative diseases. Lab Invest Jul. 01, 2019;99(7):943—57. https://doi.org/10.1038/s41374-019-0232-y. Nature Publishing Group.

[4] Basso JC, Suzuki WA. The effects of acute exercise on mood, cognition, neurophysiology, and neurochemical pathways: a review. Brain Plast Feb. 2017;2(2):127—52. https://doi.org/10.3233/bpl-160040.

[5] Van Praag H. Neurogenesis and exercise: past and future directions. Neuro-Molecular Med Jun. 2008;10(2):128—40. https://doi.org/10.1007/s12017-008-8028-z.

[6] Tsai SF, Liu YW, Kuo YM. Acute and long-term treadmill running differentially induce c-Fos expression in region- and time-dependent manners in mouse brain. Brain Struct Funct Nov. 2019;224(8):2677—89. https://doi.org/10.1007/s00429-019-01926-5.

[7] Werme M, Messer C, Olson L, Gilden L, Thoré P, Nestler E, et al. FosB regulates wheel running. J Neurosci 2002;22(18):8133—8. https://doi.org/10.1523/JNEUROSCI.22-18-08133.2002.

[8] Zhu L, Fan J, Chao F, Zhou C, Jiang L, Zhang Y, et al. Running exercise protects spinophilin-immunoreactive puncta and neurons in the medial prefrontal cortex of APP/PS1 transgenic mice. J Comp Neurol Apr 2022;530(6):858—70. https://doi.org/10.1002/cne.25252.

[9] He Y, Madeo G, Liang Y, Zhang C, Hempel B, Liu X, et al. A red nucleus-VTA glutamate pathway underlies exercise reward and the therapeutic effect of exercise on cocaine use. Sci Adv 2022;8:1440. https://doi.org/10.1126/sciadv.abo1440.

[10] Dorling J, Broom D, Burns S, Clayton D, Deighton K, James L, et al. Acute and chronic effects of exercise on appetite, energy intake, and appetite-related hormones: the modulating effect of adiposity, sex, and habitual physical activity. Nutrients Sep. 01, 2018;10(9). https://doi.org/10.3390/nu10091140. MDPI AG.

[11] King NA, Caudwell PP, Hopkins M, Stubbs JR, Naslund E, Blundell JE. Dual-process action of exercise on appetite control: increase in orexigenic drive but improvement in meal-induced satiety. Am J Clin Nutr Oct. 2009;90(4):921—7. https://doi.org/10.3945/ajcn.2009.27706.

[12] Beaulieu K, Oustric P, Finlayson G. The impact of physical activity on food reward: review and conceptual synthesis of evidence from observational, acute, and chronic exercise training studies. Current obesity reports Jun. 01, 2020;9(2): 63—80. https://doi.org/10.1007/s13679-020-00372-3. NLM (Medline).

[13] Law LF, Sluka KA. How does physical activity modulate pain? Pain 2017;158(3):369—70. https://doi.org/10.1097/j.pain.0000000000000792.

[14] Mian OS, Baltzopoulos V, Minetti AE, V Narici M. The impact of physical training on locomotor function in older people. Sports Med 2007;37(8):683—701. https://doi.org/10.2165/00007256-200737080-00003.

[15] Ashton-Miller JA, Wojtys EM, Huston LJ, Fry-Welch D. Can proprioception really be improved by exercises? Knee Surg Sports Traumatol Arthrosc 2001;9(3):128—36. https://doi.org/10.1007/s001670100208.

[16] Liu YF, Chen HI, Wu CL, Kuo YM, Yu L, Huang AM, et al. Differential effects of treadmill running and wheel running on spatial or aversive learning and memory: roles of amygdalar brain-derived neurotrophic factor and synaptotagmin I. J Physiol 2009;587(13):3221—31. https://doi.org/10.1113/jphysiol.2009.173088.

[17] Leasure JL, Jones M. Forced and voluntary exercise differentially affect brain and behavior. Neuroscience Oct. 2008;156(3):456—65. https://doi.org/10.1016/j.neuroscience.2008.07.041.

[18] Svensson M, Rosvall P, Boza-Serrano A, Andersson E, Lexell J, Deierborg T. Forced treadmill exercise can induce stress and increase neuronal damage in a mouse model of global cerebral ischemia. Neurobiol Stress Dec. 2016;5:8—18. https://doi.org/10.1016/j.ynstr.2016.09.002.

[19] Dishman RodK. Brain monoamines, exercise, and behavioral stress: animal models. Med Sci Sports Exerc 1997;21(1):63—74.

[20] Brown DA, Johnson MS, Armstrong CJ, Lynch JM, Caruso NM, Ehlers LB, et al. Short-term treadmill running in the rat: what kind of stressor is it? J Appl Physiol 2007;103:1979—85. https://doi.org/10.1152/japplphysiol.00706.2007.-The.

[21] Sherwin CM. Voluntary wheel running: a review and novel interpretation. Anim Behav 1998;56:11—27. https://doi.org/10.1006/anbe.1998.0836.

[22] Greenwood BN, Fleshner M. Voluntary wheel running: a useful rodent model for investigating mechanisms of stress robustness and exercise motivation. Current Opinion in Behavioral Sciences Aug. 01, 2019;28:78—84. https://doi.org/10.1016/j.cobeha.2019.02.001. Elsevier Ltd.

[23] Renier N, Adams EL, Kirst C, Wu Z, Azevedo R, Kohl J, et al. Mapping of brain activity by automated volume analysis of immediate early genes. Cell Jun 2016;165(7):1789—802. https://doi.org/10.1016/j.cell.2016.05.007.

[24] Alanentalo T, Asayesh A, Morrison H, Lorén CE, Holmberg D, Sharpe J, et al. Tomographic molecular imaging and 3D quantification within adult mouse organs. Nat Methods Jan 2007;4(1):31—3. https://doi.org/10.1038/nmeth985.

[25] Ertürk A, Becker C, Jährling N, Mauch CP, Hojer CD, Egen JG, et al. Three-dimensional imaging of solvent-cleared organs using 3DISCO. Nat Protoc Nov 2012;7(11):1983—95. https://doi.org/10.1038/nprot.2012.119.

[26] Ueda HR, Ertürk A, Chung K, Gradinaru V, Chédotal A, Tomancak P, et al. Tissue clearing and its applications in neuroscience. Nat Rev Neurosci Feb. 01, 2020;21(2):61—79. https://doi.org/10.1038/s41583-019-0250-1. Nature Research.

[27] Dodt HU, Leischner U, Schierloh A, Jährling N, Mauch CP, Deininger K, et al. Ultramicroscopy: three-dimensional visualization of neuronal networks in the whole mouse brain. Nat Methods Apr 2007;4(4):331—6. https://doi.org/10.1038/nmeth1036.

[28] Perens J, Hecksher-Sørensen J. Digital brain maps and virtual neuroscience: an emerging role for light-sheet fluorescence microscopy in drug development. Front Neurosci Apr. 20, 2022;16. https://doi.org/10.3389/fnins.2022.866884. Frontiers Media S.A.

[29] Renier N, Wu Z, Simon DJ, Yang J, Ariel P, Tessier-Lavigne M. iDISCO: a simple, rapid method to immunolabel large tissue samples for volume imaging. Cell 2014;159(4):896—910.

[30] Hansen HH, Perens J, Roostalu U, Skytte JL, Salinas CG, Barkholt P, et al. Whole-brain activation signatures of weight-lowering drugs. Mol Metabol May 2021:47. https://doi.org/10.1016/j.molmet.2021.101171.

[31] Skovbjerg G, Roostalu U, Hansen HH, Lutz TA, Le Foll C, Salinas CG, et al. Whole-brain mapping of amylin-induced neuronal activity in receptor activity—modifying protein 1/3 knockout mice. Eur J Neurosci Jul 2021;54(1):4154—66. https://doi.org/10.1111/ejn.15254.

[32] Perens J, Salinas CG, Skytte JL, Roostalu U, Dahl AB, Dyrby TB, et al. An optimized mouse brain atlas for automated mapping and quantification of neuronal activity using iDISCO+ and light sheet fluorescence microscopy. Neuroinformatics 2021;19(3):433—46. https://doi.org/10.1007/s12021-020-09490-8.

[33] Klein S, Staring M, Murphy K, Viergever MA, Pluim JPW. Elastix: a toolbox for intensity-based medical image registration. IEEE Trans Med Imag Jan. 2010;29(1):196—205. https://doi.org/10.1109/TMI.2009.2035616.

[34] Girard I, Garland T. Plasma corticosterone response to acute and chronic voluntary exercise in female house mice. J Appl Physiol 2002;92(4):1553—61. https://doi.org/10.1152/japplphysiol.00465.2001.

[35] Aditi M, Islam R, Kaurani L, Sakib S, Krüger DM, Burkhardt S, et al. A single-cell transcriptomic analysis of the mouse hippocampus after voluntary exercise 2 3 Aditi Methi 1#. bioRxiv Aug. 2023. https://doi.org/10.1101/2023.08.03.551761.

[36] Brümmer V, Schneider S, Strüder HK, Askew CD. Primary motor cortex activity is elevated with incremental exercise intensity. Neuroscience May 2011;181: 150—62. https://doi.org/10.1016/j.neuroscience.2011.02.006.

[37] Duvarci S, Popa D, Paré D. Central amygdala activity during fear conditioning. J Neurosci Jan. 2011;31(1):289—94. https://doi.org/10.1523/JNEUROSCI.4985-10.2011.

[38] Stevens FL, Hurley RA, Taber KH, Hayman LA. Anterior cingulate cortex: unique role in cognition and emotion. J Neuropsychiatry Clin Neurosci 2011;23(2) [Online]. Available: http://neuro.psychiatryonline.org.

[39] Gross CT, Canteras NS. The many paths to fear. Nat Rev Neurosci Sep. 2012;13(9):651—8. https://doi.org/10.1038/nrn3301.

[40] Thanawalla AR, Chen AI, Azim E. The cerebellar nuclei and dexterous limb movements. Neuroscience Dec. 01, 2020;450:168—83. https://doi.org/10.1016/j.neuroscience.2020.06.046. Elsevier Ltd.

[41] Kostadinov D, Häusser M. Reward signals in the cerebellum: origins, targets, and functional implications. Neuron Apr. 20, 2022;110(8):1290—303. https://doi.org/10.1016/j.neuron.2022.02.015. Cell Press.

[42] Hoshi E, Tremblay L, Féger J, Carras PL, Strick PL. The cerebellum communicates with the basal ganglia. Nat Neurosci Nov. 2005;8(11):1491—3. https://doi.org/10.1038/nn1544.

[43] Neudorfer C, Maarouf M. Neuroanatomical background and functional considerations for stereotactic interventions in the H fields of Forel. Brain Struct Funct Jan. 2018;223(1):17—30. https://doi.org/10.1007/s00429-017-1570-4.

[44] Dale A, Cullen KE. The nucleus prepositus predominantly outputs eye movement-related information during passive and active self-motion. J Neurophysiol 2013;16:1900—11. https://doi.org/10.1152/jn.00788.2012.-Maintaining.

[45] Gray PA. Transcription factors define the neuroanatomical organization of the medullary reticular formation. Front Neuroanat Apr. 2013;(APR). https://doi.org/10.3389/fnana.2013.00007.

[46] Sandkühler J. The organization and function of endogenous antinociceptive systems. Prog Neurobiol 1996;50:49—81. https://doi.org/10.1016/0301-0082(96)00031-7.

[47] Shimizu S, Nakatani Y, Kurose M, Imbe H, Ikeda N, Takagi R, et al. Modulatory effects of repeated psychophysical stress on masseter muscle nociception in

the nucleus raphe magnus of rats. J Oral Sci 2020;62(2):231—5. https://doi.org/10.2334/josnusd.19-0320.

[48] Taylor BK, Westlund KN. The noradrenergic locus coeruleus as a chronic pain generator. J Neurosci Res Jun. 2017;95(6):1336—46. https://doi.org/10.1002/jnr.23956.

[49] Koga K, Yamada A, Song Q, Li X, Chen Q, Liu RH, et al. Ascending noradrenergic excitation from the locus coeruleus to the anterior cingulate cortex. Mol Brain Mar 2020;13(1). https://doi.org/10.1186/s13041-020-00586-5.

[50] Kuner R, Kuner T. Cellular circuits in the brain and their modulation in acute and chronic pain. Physiol Rev Jan. 2021;101(1):213—58. https://doi.org/10.1152/physrev.00040.2019.

[51] Hunt SP, Mantyh PW. The molecular dynamics of pain control. Nature Reviews 2001;2 [Online]. Available: www.nature.com/reviews/neuro.

[52] Ennis M, Behbehani M, Shipley MT, van Bockstaele EJ, Aston-Jones G. Projections from the periaqueductal gray to the rostromedial pericoerulear region and nucleus locus coeruleus: anatomic and physiologic studies. J Comp Neurol 1991;306(3):480—94. https://doi.org/10.1002/cne.903060311.

[53] Rizzi G, Coban M, Tan KR. Excitatory rubral cells encode the acquisition of novel complex motor tasks. Nat Commun Dec. 2019;10(1). https://doi.org/10.1038/s41467-019-10223-y.

[54] Nelson AJD. The anterior thalamic nuclei and cognition: a role beyond space? Neurosci Biobehav Rev Jul. 01, 2021;126:1—11. https://doi.org/10.1016/j.neubiorev.2021.02.047. Elsevier Ltd.

[55] Myers B, McKlveen JM, Herman JP. Glucocorticoid actions on synapses, circuits, and behavior: implications for the energetics of stress. Front Neuroendocrinol 2014;35(2):180—96. https://doi.org/10.1016/j.yfrne.2013.12.003. Academic Press Inc.

[56] Bruhn T0, Plotsky PM, Valet WW. Effect of paraventricular lesions on corticotropin-releasing factor (CRF)-Like immunoreactivity in the stalk-median eminence: studies on the adrenocorticotropin response to ether stress and exogenous CRF*. Endocrinology 1984;114(1) [Online]. Available: https://academic.oup.com/endo/article/114/1/57/2538060.

[57] Garrigos D, Martínez-Morga M, Toval A, Kutsenko Y, Barreda A, Do Couto BR, et al. A handful of details to ensure the experimental reproducibility on the forced running wheel in rodents: a systematic review. Front Endocrinol May 2021;12. https://doi.org/10.3389/fendo.2021.638261.

[58] Herrera JJ, Fedynska S, Ghasem PR, Wieman T, Clark PJ, Gray N, et al. Neurochemical and behavioural indices of exercise reward are independent of exercise controllability. Eur J Neurosci May 2016;43(9):1190—202. https://doi.org/10.1111/ejn.13193.

[59] Abdul M, Yan HQ, Zhao WN, Lyu XB, Xu Z, Yu XL, et al. VTA-NAc glutaminergic projection involves in the regulation of pain and pain-related anxiety. Front Mol Neurosci Dec. 2022;15. https://doi.org/10.3389/fnmol.2022.1083671.

[60] Harris H, Peng Y. Evidence and explanation for the involvement of the nucleus accumbens in pain processing. Neural Regen Res Apr. 2020;15(4):597—605. https://doi.org/10.4103/1673-5374.266909.

[61] Rhodes JS, Garland T, Gammie SC. Patterns of brain activity associated with variation in voluntary wheel-running behavior. Behav Neurosci Dec. 2003;117(6):1243—56. https://doi.org/10.1037/0735-7044.117.6.1243.

[62] Ulrich-Lai YM, Herman JP. Neural regulation of endocrine and autonomic stress responses. Nat Rev Neurosci Jun. 2009;10(6):397—409. https://doi.org/10.1038/nrn2647.

[63] Godoy LD, Rossignoli MT, Delfino-Pereira P, Garcia-Cairasco N, Umeoka EH de L. A comprehensive overview on stress neurobiology: Basic concepts and clinical implications. Front Behav Neurosci Jul. 03, 2018;12. https://doi.org/10.3389/fnbeh.2018.00127. Frontiers Media S.A.

